Available online at www.sciencedirect.com

ScienceDirect

Procedia Structural Integrity 33 (2021) 704–713

Structural Integrity Procedia

www.elsevier.com/locate/procedia

IGF26 - 26th International Conference on Fracture and Structural Integrity

Preliminary Finite Element assessment of residual stresses in dissimilar AA6082-S355 butt welded joints produced with the Hybrid Metal Extrusion and Bonding (HYB) technique

Francesco Leoni*[a], Paolo Ferro[b], Filippo Berto[a]

[a]*Department of Mechanical and Industrial Engineering, NTNU, Richard Birkelands vei 2b, 7491 Trondheim, Norway*
[b] *Department of Management and Engineering, University of Padova, Stradella S. Nicola, 2 I-36100 Vicenza, Italy*

Abstract

Hybrid Metal Extrusion & Bonding (HYB) is a new solid-state joining method for metals and alloys that utilizes continuous extrusion as a technique to enable aluminum filler metal additions. Previous works showed that this method is well suitable for joining dissimilar metals such as steel and aluminum. In the present paper a Finite Element model for the thermal residual stresses were implemented employing the FE code WELDSIM. As a starting point, the results of a semi-analytical heat generation model previously implemented for HYB process of aluminum butt welds were used to estimate the net power input as a sum of contributions that are dependent on the welding parameters i.e. the welding speed, the rotational speed and the material properties. Subsequently, the thermal stresses occurring in the material and finally the residual stresses were determined. In the present work, predictions of the FE model for different sets of welding parameters are presented and discussed.

Keywords: Aluminium alloys; Structural Steel; FEM; Dissimilar welds; Heat flow modelling; HYB; Residual Stresses.

* Corresponding author. Tel.: +393473335042
E-mail address: francesco.leoni@ntnu.no

2452-3216
10.1016/j.prostr.2021.10.078

1. Introduction

Energy and environmental preservation are critical issues that must be addressed, and decreasing vehicle weight through good material selection and the development of joining techniques are effective ways to reduce fuel consumption (Coelho et al., 2012; Ermolaeva et al., 2004; Kochan, 2002; Michalos et al., 2010). During the last few decades, there has been a rise in interest in joining steel and aluminum alloys in both science and automotive fields (Chen and Kovacevic, 2004; Coelho et al., 2008; Lee et al., 2006; Springer et al., 2011; Tanaka et al., 2009; Uzun et al., 2005; Watanabe et al., 2006). Many designers and engineers are attracted to hybrid structures that combine the high strength, good formability, and creep resistance of steels with the low density, excellent corrosion resistance, and high thermal conductivity of aluminum alloys. Although much work has been done to weld steel to aluminum alloy, sound connections are still difficult to achieve using traditional fusion welding techniques. The low solubility of Fe in Al, which is close to zero at ambient temperature, is one of the key challenges in joining these two metals. Furthermore, at high temperatures, the solid solubility limit of Fe in Al is very low, leading in welding defects such as solidification and liquidation cracks, as well as porosity, making the production of sound joints challenging (Dehghani et al., 2013). Moreover, under the high temperatures of fusion welding techniques, the refractory Al_2O_3 oxide film is easy to form on the surface of aluminum alloy, resulting in slag inclusion in the weld and, as a result, joint performance loss. Another issue to consider is the fact that liquid aluminum alloy has poor wetting and spreading properties when applied on uncoated steel sheets (Wan and Huang, 2018). Furthermore, differences in melting temperature, thermal properties, and cooling rate after welding of both metallic alloys are issues that affect the bond quality, particularly with traditional fusion welding processes that involve high temperatures. Furthermore, the interfacial zone of Al-steel joint is prone to generate brittle intermetallic compounds (IMCs) such as $FeAl_2$, $FeAl_3$, Fe_2Al_5 which lead to crack formation when combined with tension arising from welding residual stresses leading to a weak joint (Liu et al., 2015). To summarize, the mechanical properties of Al-steel joints can be strongly influenced by the growth of brittle IMCs, which are formed during the interfacial reaction between solid steel and liquid aluminum. For all these reasons, new methods are needed to realize the rapid development of the welding of dissimilar aluminum alloys and steels.

During last decades, a lot of effort has been spent in finding a suitable solid-state process for the production of sound Al-steel joints. The methods include friction stir knead welding (Geiger et al., 2008), friction welding (Sahin, 2009; Taban et al., 2010), surface activated bonding (Howlader et al., 2010), abrasion circle friction spot welding (Chen et al., 2012), cold metal transfer (Cao et al., 2013) and barrel nitriding process (Kong et al., 2014). However, the high cost and the special equipment that those techniques require are still limiting factors to consider.

Recently, a new solid-state joining method for metals and alloys has been developed, known as the Hybrid Metal Extrusion and Bonding (HYB) process (Leoni et al., 2021, 2020a, 2020b). This method, which is based on the principles of continuous extrusion, allows joining to be performed using aluminum filler metal (FM) additions similar to that done in gas metal arc welding (GMAW) but without any melting involved (see Fig.1). In recent years, the first generation of Al-steel HYB butt joint was investigated and promising results were reported (Berto et al., 2018). More recently, a work on the second generation Al-steel HYB butt joint that was subjected to microstructural and mechanical characterization has been published (Bergh et al., 2020). In the cited work, Bergh et al. found that the Al-steel HYB butt joint showed considerable bond strength that was attributed to a combination of microscale mechanical interlocking and a nanoscale interfacial Al-Fe-Si layer. In their work, they found that the quality of the weld increased compared to what previously reported by Berto et al. (Berto et al., 2018), showing how the different welding setup can largely affect the joint quality. In particular, they attributed the increasing in the bond strength to two main factors: the shape of the steel groove and the position of the hardest material on the AS instead of on the RS. The first generation had a half V-form and the steel was placed on the RS while the second generation had a half Y-form and the steel was placed on the AS. This change was consistent with the standard practice of placing the hardest material on the AS for FSW butt joints because it is known that the material on the AS experiences larger shear forces, which gives better Al-steel bonding. From these previous works one can conclude that small changes in the welding setup can bring to large differences in the joint quality. So far, regarding the second generation of Al-steel HYB butt joint, only one welding condition was investigated, leaving unknown the dependency of the weld quality to the main process parameters.

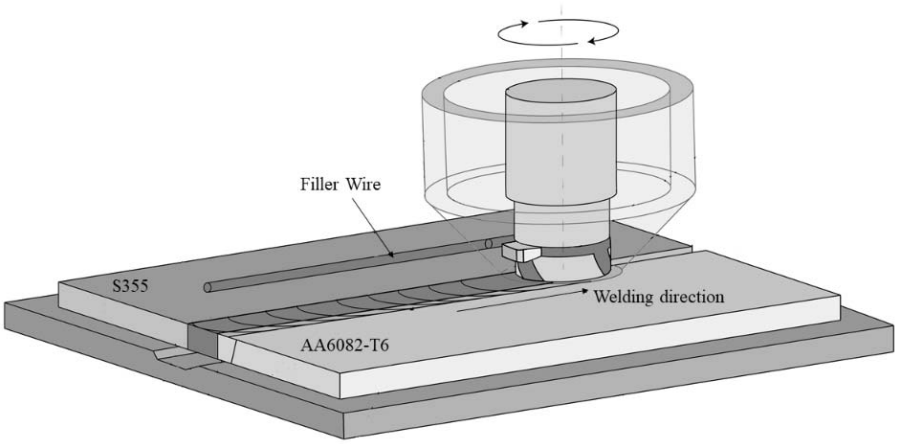

Fig. 1: Schematic illustration of Al-steel HYB butt joining. The plates are clamped onto a steel backing, with Al on the retreating side (RS) and steel on the advancing side (AS). During operation, the HYB PinPoint extruder moves along the joint line, continuously extruding Aluminum Filler Material through the rotating dies of the pin. The bond is formed when the Al FM fully fills the groove.

As mentioned above, an important aspect to consider when dealing with welding processes are residual stresses, which are a consequence of heating and cooling cycles occurring in the joint and in the parent material. The localized heating induced by welding results in non-uniform temperature fields, which are associated with thermal expansion and contraction of the metal. It is well known that residual tensile stresses can contribute to brittle fractures or cause premature failures in components subjected to fatigue (Foti et al., 2019; Foti and Berto, 2020), while compression stresses are responsible for deformations and buckling in thin large panels, such as those used in the automotive industry. For these reasons, the assessment of magnitude and distribution of residual stresses can be extremely helpful in the design phase of a welded structure (Barsoum and Barsoum, 2009; Dong, 2005; Leggatt, 2008; Masubuchi, 2013; Sandnes, 2018).

In the past, welding residual stress investigation employed only experimental measurement methods. However, all these experimental techniques are time-consuming and unable to capture the complete stress distributions. In recent years, the development of numerical Finite Element codes made it possible to simulate the whole welding process considering all the related effects such as precipitates dissolution, solid-state phase transformation, elastic-plastic and creep behavior of the material under investigation.

In the present study, the authors explored the second generation of Hybrid Metal Extrusion and Bonding (HYB) of AA6082-S355 with a finite element approach and investigated the effects of the main process parameters on the residual stresses. The results presented herein will be used to better choose future sets of experimental setups.

2. Materials and Methods

2.1. Geometry

Fig. 2 shows the dimensions of the geometry together with the mesh used. A finer mesh was modelled in the vicinity of the weld line to account for the higher thermal and stress gradients that occurs in this zone.

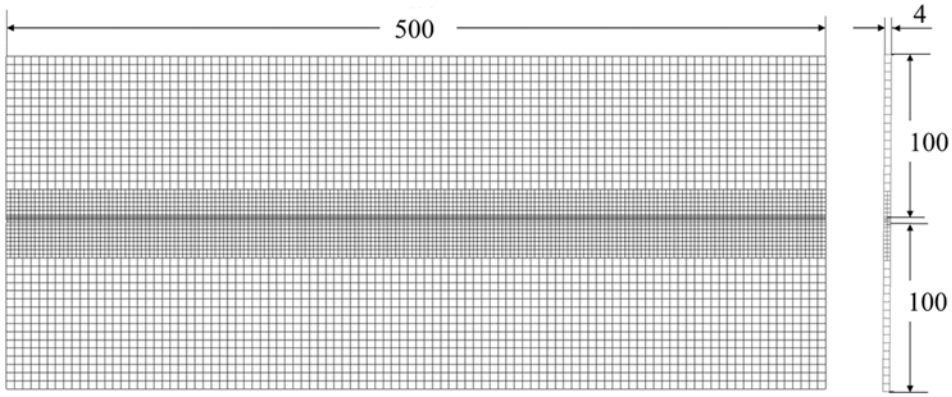

Fig.2: Schematic representation of the weld modelled with the corresponding measures and mesh used for the FE simulations.

2.2. Material properties

The material properties implemented in the model for the steel plate are shown in Fig. 3, while the ones used for the Aluminum side are shown in Fig. 4.

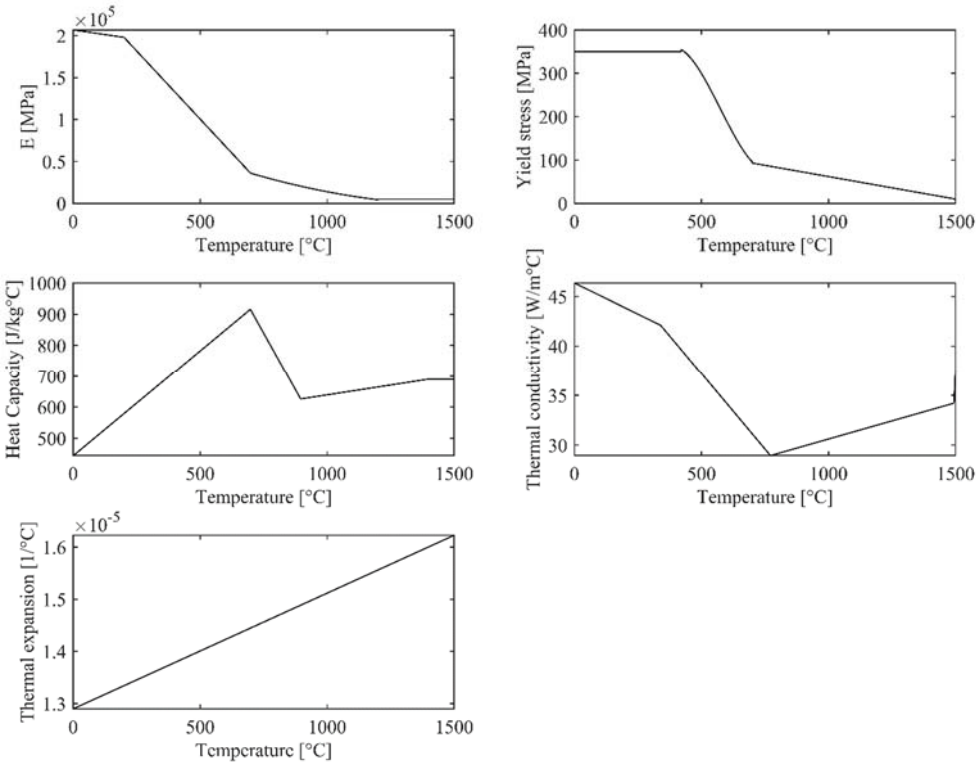

Fig. 3: Temperature-dependent material properties of S355. Data of Heat Capacity, Thermal Conductivity and Thermal expansion were taken from (Zhu et al., 2019).

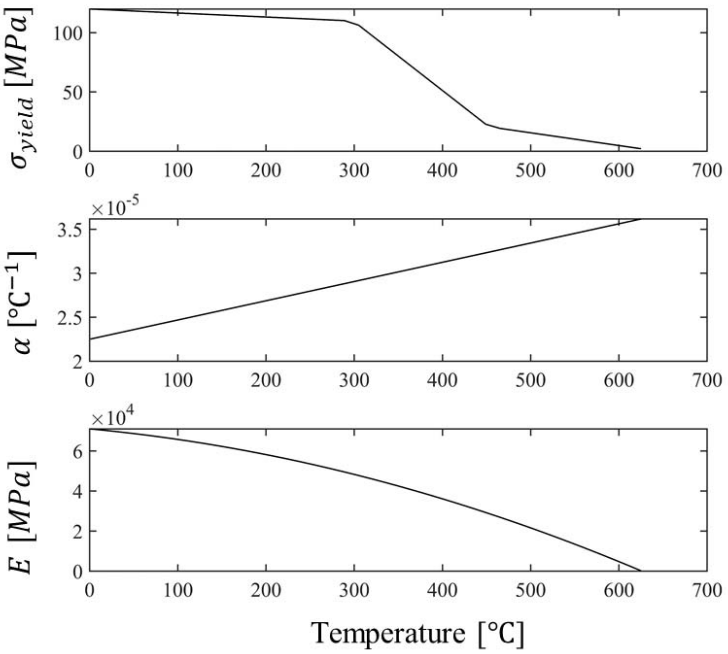

Fig.4: Temperature-dependent material properties of AA6082.

2.3. Numerical modeling

First, the thermal simulation of the process was run to obtain temperature fields in accordance to experimental records of similar welding setups previously calibrated for aluminum butt welds. Once the model was considered calibrated from the thermal point of view, mechanical stage to get thermal-induced stresses and deformations were conducted. The independent process parameters levels taken into consideration for the present preliminary study are summarized in Table 1 while the simulated conditions are summarized in Table 2.

Table 1: Process parameters levels being investigated.

	Level 1	Level 2	Level 3
Welding speed (mm/s)	8	12	16
Rotational speed (RPM)	350	350	350

Table 2: Simulation layout.

Condition	**Welding speed (level)**	**Rotational speed (level)**
1	1	1
2	2	1
3	3	1

2.4. Heat generation model

The heat source has been modeled as a double ellipsoid along the weld bead. The energy of heat source q_0 (W) was extrapolated from (Leoni et al., 2021). In brief, the model employed used an adaptive adjustment of the friction coefficient that takes into consideration the temperature at the tool matrix interface and adjusted the heat generated in order to obtain a condition of balance between the heat generated and the temperature reached. Indeed if one consider a heat generation which is too high for the welding speed considered, would found a local temperature field too high for the material to be in solid state, but if the material undergoes to melt, then the hypothesis of friction between the tool and the matrix would not be verified anymore. Instead, the balance between the local temperature and the heat generated at each welding speed has to be satisfied, and the model adopted in the present investigation is believed to describe with a reasonable degree of accuracy this effect.

2.5. Thermal Model

A backing plate was modelled to simulate the heat conduction that occurs between the plates and the backing welding table. Both the BMs plates and backing plate shared the same length and width. The boundary conditions are represented by heat transfer coefficients between the material and the environment. The top and bottom surfaces of the workpiece are assumed to have two different heat convection coefficients. At the top surface, a convective heat transfer coefficient of 20 Wm^{-2} K^{-1} was used. The value is typical for natural convection between aluminum and air. At the bottom surface of the workpiece, a conductive heat transfer of 200 Wm^{-1} K^{-1} was set between the two domains (i.e. the plates and the backing table). To simulate the heat generation associated with friction and hot material extrusion, the welding heat source was modeled as a double ellipsoid volume distributed heat source as proposed by Goldak et al. (Goldak et al., 1984), positioned in the middle of the two workpieces. This heat source moves along the weld line in the mid-thickness of the workpiece at the same speed as the tool, i.e. at 8 and 12 and 16 mm/s. To account for the metal deposition from the PinPoint extruder, elements that form the weld were continuously activated during welding as the heat source proceeds along the weld. Furthermore, in order to obtain the correct heat capacity of the part, the density of the filler metal has been adjusted to account for the excess of material present in the real joining procedure compared to the ideally smooth weld profile being modelled.

2.6. Mechanical Model

Fig. 5 shows the mechanical boundary conditions and their corresponding locations. The only forces considered herein were the ones due to thermal expansion. Unclamping was considered employing a time dependent mechanical boundary condition, which deactivated the normal stiffness at the edges of the plates after cooling.

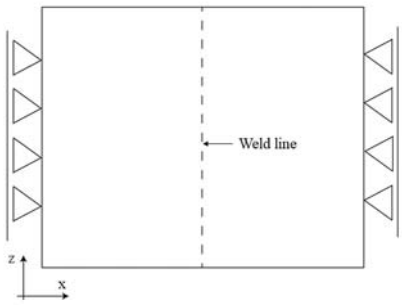

Fig. 5: Mechanical Boundary conditions.

3. Results and discussion

3.1. Thermal field

Fig. 6 shows the thermal field arising during dissimilar HYB welding. The thermal gradient is much higher in the steel side because of the lower thermal conductivity that characterizes this zone, while in the aluminum side, having a much higher thermal conductivity coefficient the heat is transferred much faster and creates a wider and less steep gradient. This is shown also in Fig. 7, where the evolution of temperature during time in a cross section taken at the mid-length of the plates was considered. As can be seen the gradient in the steel side is greater than that on the aluminum side, and this causes the aluminum side to be subjected to plasticization in a wider zone since the thermal softening occurs for a greater portion of material. This phenomenon affects the thermal stresses distribution, creating a wider zone where the gradient is lower whereas where the gradient is greater the stresses are localized in a narrower zone. This effect is shown in Fig. 9.

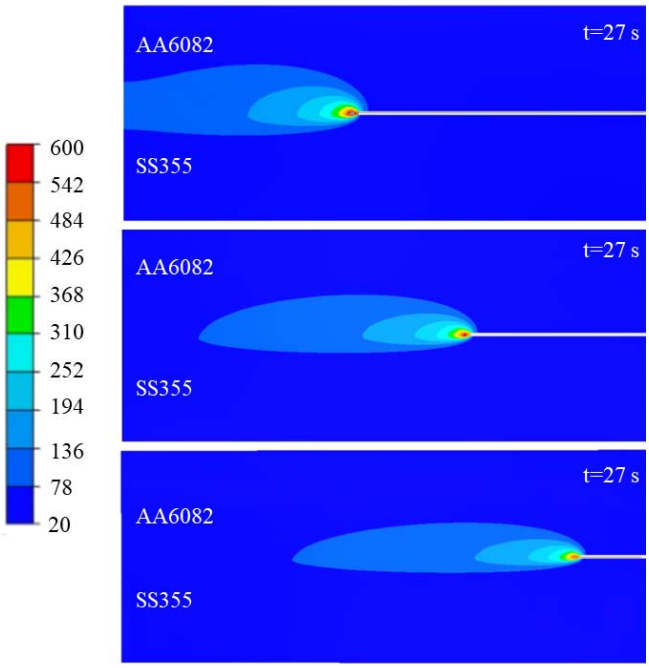

Fig.6: Contour plots showing the thermal field (˚C) during welding operation of aluminum-steel for the welding speeds of 8, 12 and 16 mm/s and for the power inputs of 900, 1000 and 1100 W respectively.

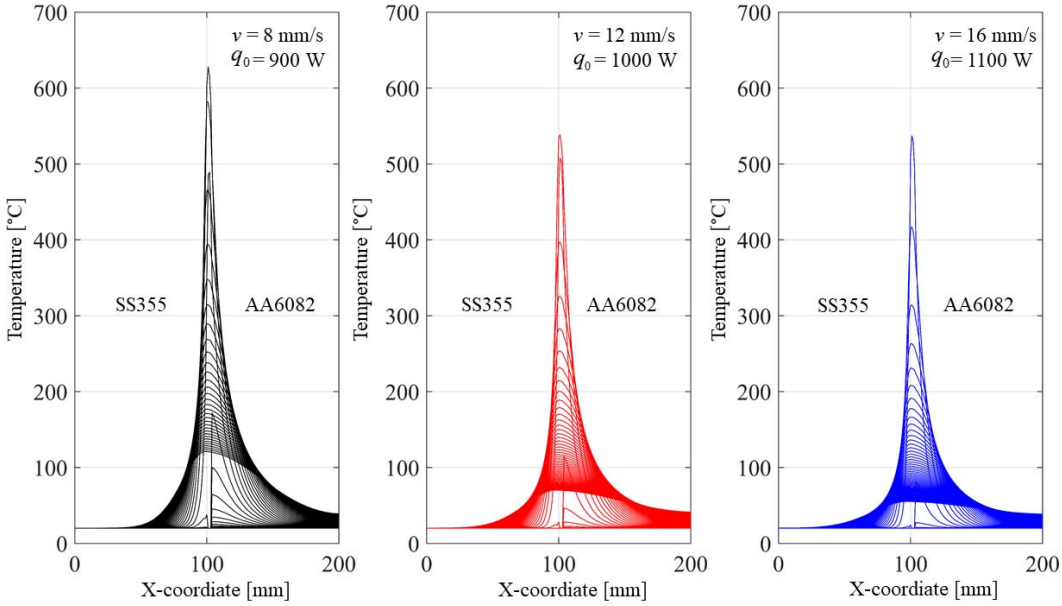

Fig. 7: Evolution of temperature for the three welding velocities and for the respective heat input of a transverse cross section taken at the mid-length of the plates.

3.2. Thermal and residual stresses

Fig. 8 shows the evolution of longitudinal stress during cooling. As expected, in the zone that does not undergo plastic deformation, the stress starts to decrease until the balance between stresses due to the plasticized zone in the vicinity of the weld line are balanced by the elastic response of the cold unyielded material.

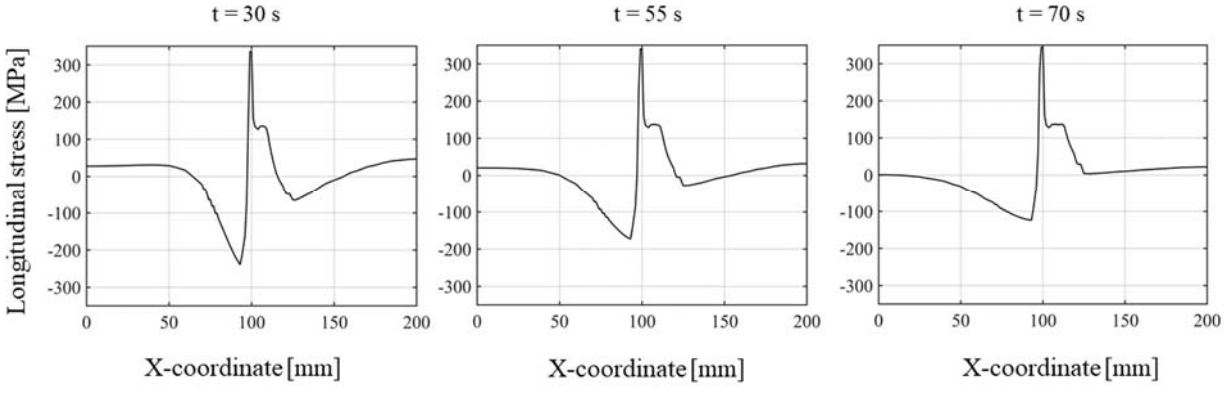

Fig. 8: Evolution of longitudinal thermal stresses during cooling considering a cross section at the mid-length of the plates being welded.

Finally, Fig. 9 displays longitudinal residual stress distribution at the middle length of the plates calculated by the finite element model for the welding speed of 8, 12 and 16 mm/s and a heat input of 900, 1000 and 1100 W respectively.

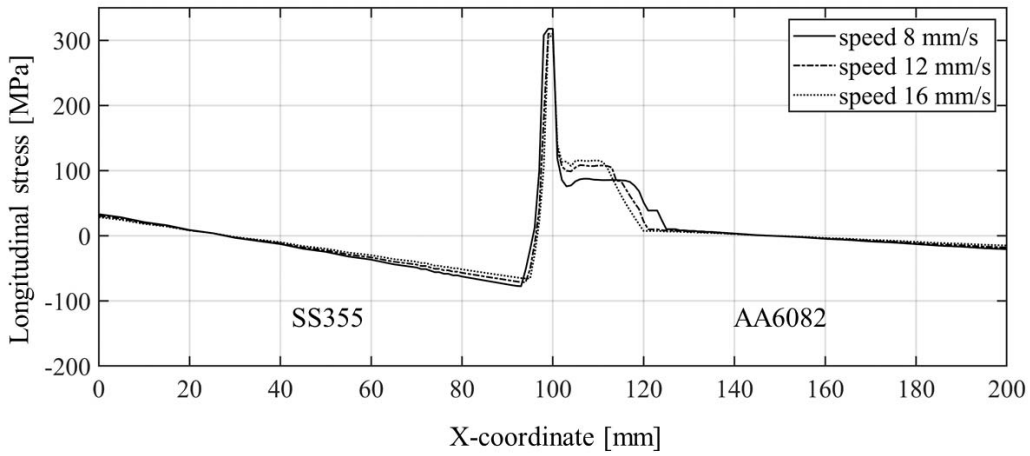

Fig. 9: Longitudinal stresses for different welding velocities.

4. Conclusions

This study conducted the estimation of thermal residual stresses of HYB butt welds of dissimilar S355-AA6082 plates by means of a Finite Element model. The model was used to compare the results for different welding setups, in particular, the influence of the welding speed on transverse residual stresses was studied. The non-symmetric stress field typical for dissimilar joints was found and from the study it can be concluded that the transverse residual stresses of the weld are lower for higher welding speeds but not as much as one would expect considering common fusion welds. This because in HYB process the power used by the machine is proportional to the welding speed used. This phenomenon was observed for aluminum butt welds and the same can be expected for the current dissimilar metal case. The physical framework behind this behavior is attributed to the fact that the torque needed to plastically deform the parent material is grater for lower temperatures, which actually tend to be lower when one welds at higher speeds. This effect on the other side causes a higher torque being applied and consequently a higher heat input to consider when one models the process. In conclusion, despite this mitigating effect typical for friction driven processes, it can be said that higher welding speeds produce a narrower zone of residual stress, but this beneficial aspect has to be further investigate with experimental measurements. At present, experimental measurements of residual stresses of HYB welds are still missing but some work is in progress. The purpose of the present investigation is to present preliminary results using data currently available that permits a quite good reliability at least from the thermal point of view. The presented simulations will be then better calibrated as experimental validations will be available.

Acknoledgements

The authors gratefully acknowledge Hallvard Gustav Fjær's assistance in the use of the WELDSIM FE code.

References

Barsoum, Z., Barsoum, I., 2009. Residual stress effects on fatigue life of welded structures using LEFM. Eng. Fail. Anal. 16, 449–467.

Bergh, T., Sandnes, L., Johnstone, D.N., Grong, Ø., Berto, F., Holmestad, R., Midgley, P.A., Vullum, P.E., 2020. Microstructural and mechanical characterisation of a second generation hybrid metal extrusion & bonding aluminium-steel butt joint. Mater. Charact. 110761.

Berto, F., Sandnes, L., Abbatinali, F., Grong, Ø., Ferro, P., 2018. Using the Hybrid Metal Extrusion & Bonding (HYB) Process for Dissimilar Joining of AA6082-T6 and S355. Procedia Struct. Integr. 13, 249–254.

Cao, R., Yu, G., Chen, J.H., Wang, P.-C., 2013. Cold metal transfer joining aluminum alloys-to-galvanized mild steel. J. Mater. Process. Technol. 213, 1753–1763.

Chen, C.M., Kovacevic, R.Ã., 2004. Joining of Al 6061 alloy to AISI 1018 steel by combined effects of fusion and solid state welding. Int. J.

Mach Tools Manuf 44, 1205–1214.
Chen, Y.C., Gholinia, A., Prangnell, P.B., 2012. Interface structure and bonding in abrasion circle friction stir spot welding: a novel approach for rapid welding aluminium alloy to steel automotive sheet. Mater. Chem. Phys. 134, 459–463.
Coelho, B.R.S., Kostka, A., Santos, J.F., Pyzalla, A.R., 2008. EBSD Technique Visualization of Material Flow in Aluminum to Steel Friction-Stir Dissimilar Welding. Adv. Eng. Mater. 1127–1133.
Coelho, R.S., Kostka, A., Santos, J.F., Kaysser-pyzalla, A., 2012. Materials Science & Engineering A Friction-stir dissimilar welding of aluminium alloy to high strength steels : Mechanical properties and their relation to microstructure. Mater. Sci. Eng. A 556, 175–183.
Dehghani, M., Amadeh, A., Mousavi, S.A.A.A., 2013. Investigations on the effects of friction stir welding parameters on intermetallic and defect formation in joining aluminum alloy to mild steel. Mater. Des. 49, 433–441.
Dong, P., 2005. Residual stresses and distortions in welded structures: a perspective for engineering applications. Sci. Technol. Weld. Join. 10, 389–398.
Ermolaeva, N.S., Castro, M.B.G., Kandachar, P. V, 2004. Materials selection for an automotive structure by integrating structural optimization with environmental impact assessment. Mater. Des. 25, 689–698.
Foti, P., Berto, F., 2020. Evaluation of the effect of the TIG-dressing technique on welded joints through the strain energy density method. Procedia Struct. Integr. 25, 201–208.
Foti, P., Berto, F., Filippi, S., 2019. Fatigue assessment of welded joints by means of the Strain Energy Density method: Numerical predictions and comparison with Eurocode 3: Numerical predictions and comparison with Eurocode 3. Frat. ed Integrità Strutt. 13, 104–125.
Geiger, M., Micari, F., Merklein, M., Fratini, L., Contorno, D., Giera, A., Staud, D., 2008. Friction Stir Knead Welding of steel aluminium butt joints. Int. J. Mach. Tools Manuf. 48, 515–521.
Goldak, J., Chakravarti, A., Bibby, M., 1984. A new finite element model for welding heat sources. Metall. Trans. B 15, 299–305.
Howlader, M.M.R., Kaga, T., Suga, T., 2010. Investigation of bonding strength and sealing behavior of aluminum/stainless steel bonded at room temperature. Vacuum 84, 1334–1340.
Kochan, A., 2002. A time of change for welding. Assem. Autom 22, 29–35.
Kong, J.H., Okumiya, M., Tsunekawa, Y., Yun, K.Y., Kim, S.G., Yoshida, M., 2014. A novel bonding method of pure aluminum and SUS304 stainless steel using barrel nitriding. Metall. Mater. Trans. A 45, 4443–4453.
Lee, W., Schmuecker, M., Mercardo, A., Biallas, G., Jung, S., 2006. Interfacial reaction in steel – aluminum joints made by friction stir welding. Scr. Mater. 55, 355–358.
Leggatt, R.H., 2008. Residual stresses in welded structures. Int. J. Press. Vessel. Pip. 85, 144–151.
Leoni, F., Grong, Ø., Ferro, P., Berto, F., 2020a. Simulating the dependence of the filler wire feeding on the wire size in the hybrid metal extrusion & bonding (HYB) process. Procedia Struct. Integr. 26, 321–329.
Leoni, F., Grong, Ø., Ferro, P., Berto, F., 2021. A Semi-Analytical Model for the Heat Generation during Hybrid Metal Extrusion and Bonding (HYB). Materials (Basel). 14.
Leoni, F., Grong, Ø., Fjær, H.G., Ferro, P., Berto, F., 2020b. A First Approach on Modelling the Thermal and Microstructure Fields During Aluminium Butt Welding Using the HYB PinPoint Extruder. Procedia Struct. Integr.
Liu, W., Ma, J., Atabaki, M.M., Kovacevic, R., 2015. Joining of advanced high-strength steel to AA 6061 alloy by using Fe/Al structural transition joint. Mater. Des. 68, 146–157.
Masubuchi, K., 2013. Analysis of welded structures: residual stresses, distortion, and their consequences. Elsevier.
Michalos, G., Makris, S., Papakostas, N., Mourtzis, D., Chryssolouris, G., 2010. Automotive assembly technologies review : challenges and outlook for a flexible and adaptive approach. CIRP J. Manuf. Sci. Technol. 2, 81–91.
Sahin, M., 2009. Joining of stainless-steel and aluminium materials by friction welding. Int. J. Adv. Manuf. Technol. 41, 487–497.
Sandnes, L., 2018. Exploring the hybrid metal extrusion and bonding process for butt welding of Al–Mg–Si alloys. Int. J. Adv. Manuf. Technol. 98, 1059–1065.
Springer, H., Kostka, A., Santos, J.F., Raabe, D., 2011. Influence of intermetallic phases and Kirkendall-porosity on the mechanical properties of joints between steel and aluminium alloys. Mater. Sci. Eng. A 528, 4630–4642.
Taban, E., Gould, J.E., Lippold, J.C., 2010. Dissimilar friction welding of 6061-T6 aluminum and AISI 1018 steel: Properties and microstructural characterization. Mater. Des. 31, 2305–2311.
Tanaka, T., Morishige, T., Hirata, T., 2009. Comprehensive analysis of joint strength for dissimilar friction stir welds of mild steel to aluminum alloys. Scr. Mater. 61, 756–759.
Uzun, H., Dalle, C., Argagnotto, A., Ghidini, T., Gambaro, C., 2005. Friction stir welding of dissimilar Al 6013-T4 To X5CrNi18-10 stainless steel. Mater. Des. 26, 41–46.
Wan, L., Huang, Y., 2018. Friction stir welding of dissimilar aluminum alloys and steels: a review. Int. J. Adv. Manuf. Technol. 99, 1781–1811.
Watanabe, T., Takayama, H., Yanagisawa, A., 2006. Joining of aluminum alloy to steel by friction stir welding. J. Mater. Process. Technol. 178, 342–349.
Zhu, J., Khurshid, M., Barsoum, Z., 2019. Accuracy of computational welding mechanics methods for estimation of angular distortion and residual stresses. Weld. World 63, 1391–1405.